Multidimensional ecological filtering shapes a specialized yet potentially flexible pollination interaction

Supplementary Materials:

Tables 1-4

Figures 1-8

Table S1. Insect visitors to *Cypripedium bardolphianum* recorded through field observations from 2004 to 2018 (* indicates species observed carrying pollinia)

Order and Family	Species
HYMENOPTERA	
Formicidae	*Formica sp.**
DIPTERA	
Syrphidae	*Melanostoma scalare*
Anthocoridae	*Lasiomma sp.*
Calliphoridae	*Calliphora vomitoria*
Drosophilidae	*Leucophenga sp.**
	*Drosophila curviceps**
	*Drosophila immigrans**
HOMOPTERA	
Cicadellidae	*Amrasca sp.*

Table S2. Species and sex of pollinators carrying *C. bardolphianum* pollinia recorded via banana-baited traps and manual capture between 2011 and 2018.

Voucher	Species	Gender	Collection site
#201101	*Formica uralensis*	--	Trap, Huanglong valley
#201102	*Formica uralensis*	--	Trap, Huanglong valley
#201103	*Drosophila immigrans*	Female	Trap, Huanglong valley
#201104	*Drosophila immigrans*	Female	Trap, Huanglong valley
#201105	*Drosophila immigrans*	Female	Trap, Huanglong valley
#201106	*Drosophila immigrans*	Female	Trap, Huanglong valley
#201107	*Leucophenga* sp.	--	Trap, Huanglong valley
#201108	*Drosophila immigrans*	Female	Trap, Huanglong valley
#201601	*Drosophila immigrans*	Female	Trap, Huanglong valley
#201602	*Drosophila immigrans*	Female	Trap, Huanglong valley
#201603	*Drosophila immigrans*	Female	Trap, Huanglong valley
#201604	*Drosophila immigrans*	Female	Trap, Huanglong valley
#201605	*Drosophila immigrans*	Female	Trap, Huanglong valley
#201606	*Drosophila immigrans*	Female	Field, Huanglong valley
#201607	*Drosophila immigrans*	Male	Field, Huanglong valley
#201608	*Drosophila curviceps*	Female	Trap, Huanglong valley
#201609	*Drosophila curviceps*	Female	Trap, Huanglong valley
#2017-1-P	*Drosophila curviceps*	Female	Trap, Huanglong valley
#2017-2-P	*Drosophila immigrans*	Female	Trap, Huanglong valley
#2017-3-P	*Drosophila immigrans*	Female	Trap, Huanglong valley
#2017-4-P	*Drosophila immigrans*	Female	Trap, Huanglong valley
#2018-1-P	*Drosophila immigrans*	Female	Trap, Huanglong valley

#2018-2-P	*Drosophila curviceps*	Female	Trap, Huanglong valley
#2018-3-P	*Drosophila immigrans*	Female	Trap, Huanglong valley

Table S3. The CAS number and other information of the identified eight volatile organic compounds (VOCs) that repeatedly detected in *C. bardolphianum*

Compound	Company	Catalog	Retention Index (RI)		CAS number
			Polar column	Non-polar column	
acetoin	S.A.	A1795-1	1305	720	513-86-0
ethyl butyrate	S.A.	E15701	1029	802	105-54-4
isobutyl acetate	S.A.	537470	1035	781	110-19-0
2,3-butanediol	S.A.	B84904	1542	778	513-85-9
3-octanone	S.A.	13691-3	1261	984	106-68-3
6-methyl-5-hepten-2-one	S.A.	M4880-5	1240	975	110-93-0
1-hexanol	S.A.	73117-1	1363	867	111-27-3
ethyl tiglate	S.A.	W24601-8	1231	949	5837-78-5

Table S4. Amounts of the 8 different floral volatiles collected from *Cypripedium bardolphianum* over three years (n=16; from 2012, 2016, 2017).

Volatiles	Chemical group	Formula	Amount (μg/ hr/ sample)	Volume ($\times 10^{-3}$ μl/sample)	Ratio of volume
Acetoin	FAD	$C_4H_8O_2$	6.4163±3.5449	6.2969±3.5036	70.80%
Ethyl butyrate	FAD	$C_6H_{12}O_2$	0.7461±0.5245	0.7945±0.5936	8.93%
6-methyl-5-Hepten-2-one	FAD	$C_5H_{12}O_2$	0.1862±0.1082	0.2161±0.1267	2.43%
Isobutyl acetate	FAD	$C_6H_{12}O_2$	0.3489±0.2731	0.3988±0.3121	4.48%
Ethyl tiglate	FAD	$C_7H_{12}O_2$	0.5790±0.2984	0.6273±0.3233	7.05%
2,3-Butanediol	FAD	$C_4H_{10}O_2$	0.1712±0.1100	0.1483±0.1083	1.67%
1-Hexanol	FAD	$C_6H_{14}O$	0.1082±0.0795	0.1320±0.0969	1.48%
3-Octanone	FAD	$C_8H_{16}O$	0.2306±0.1993	0.2806±0.2425	3.15%

Identification of these volatile compounds was confirmed by checking NIST 2011b MS Library SW Kit (Agilent Technologies) and mass spectra with co-injected authentic standards. FAD, fatty acid derivative. The mass spectra of the compounds are presented in Figure S2.

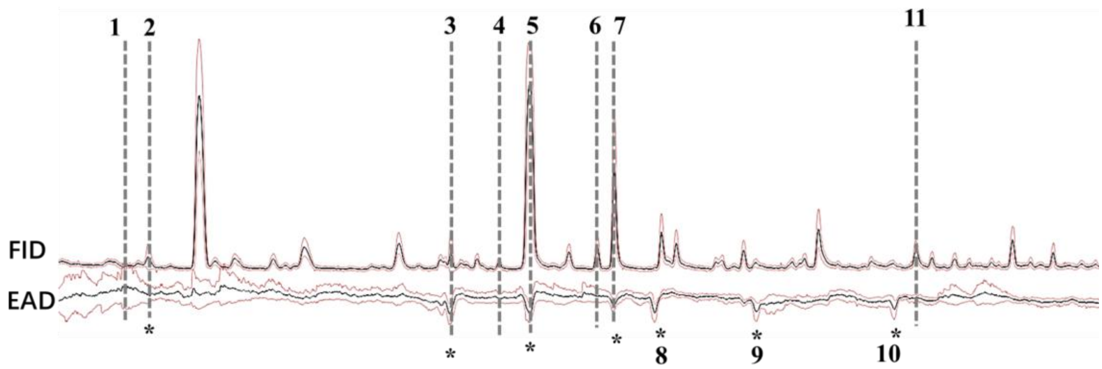

Fig. S1 GC-FID-EAD analysis of the headspace odor of *Cypripedium bardolphianum* (up trace) and electroantennographic detection (EAD) from females of *Drosophila immigrans*. The test odor sample is mixed from four field scent samples and ten times concentrated. Asterisk (*) in the EAD-trace refers to peaks eliciting antennal reactions. The VOCs denoted by these numbers are 1(ethyl isobutyrate); 2 (ethyl butyrate); 3 (ethyl tiglate); 4 (3-octanone); 5 (acetoin); 6 (6-methyl-5-heptene-2-one); 7 (1-hexanol); 8 (acetoin derivatives (acetoin acetate), also exists in acetoin reference standard); 9 (trace amount of unknown compounds that did not detect in single samples); 10 (trace amount of unknown compounds that did not detect in single samples); 11 (2,3-butanediol). (n=3)

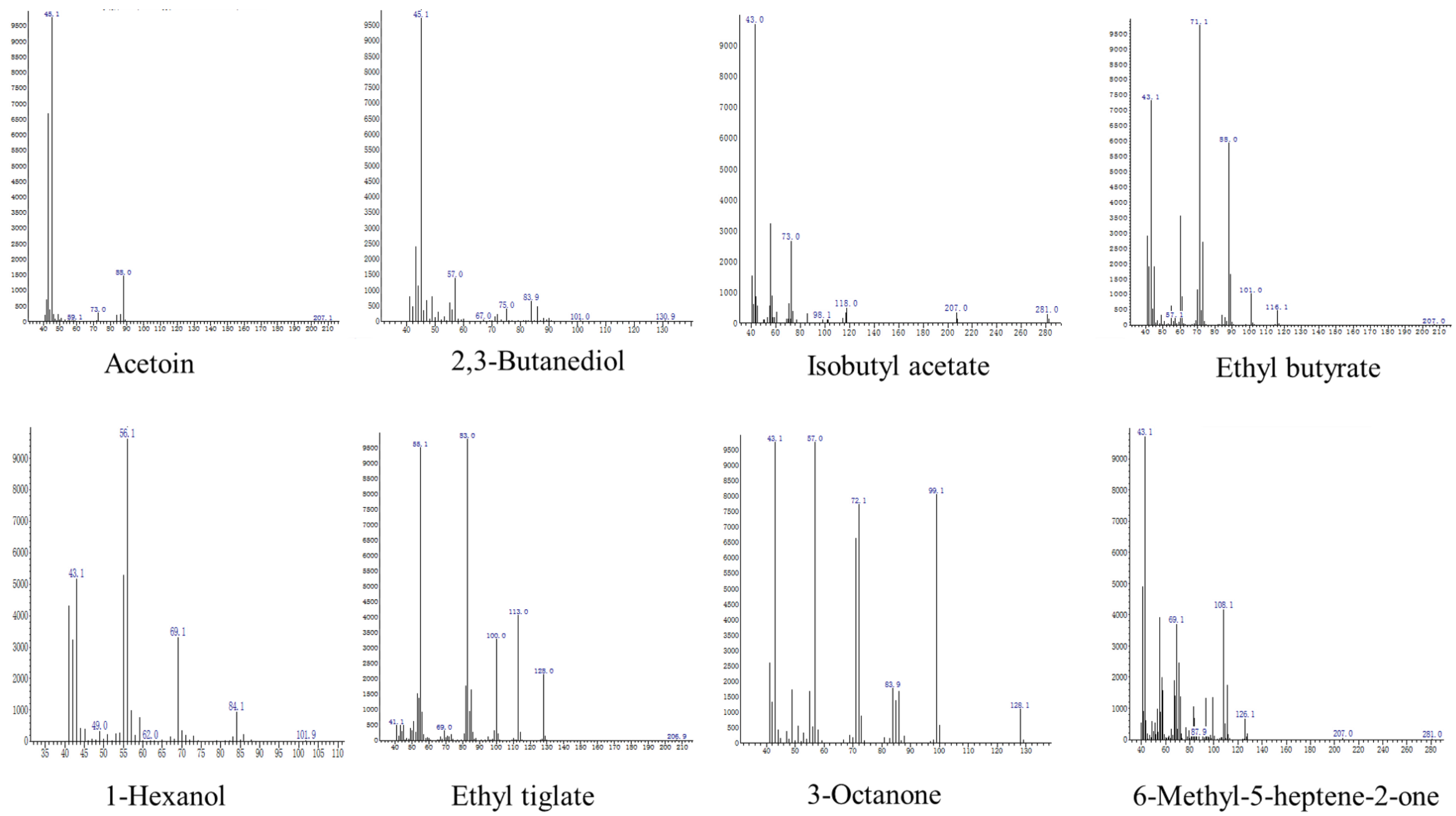

Fig. S2 Mass spectra of eight volatile organic compounds (VOCs) emitted by *Cypripedium bardolphianum*. Spectra were acquired using electron impact (EI) ionization at 70 eV. The x-axis represents the mass-to-charge ratio (m/z), and the y-axis indicates relative abundance. Compound identification was confirmed by comparing the acquired mass spectra and retention indices (RI) with the NIST mass spectral library and authentic reference standards.

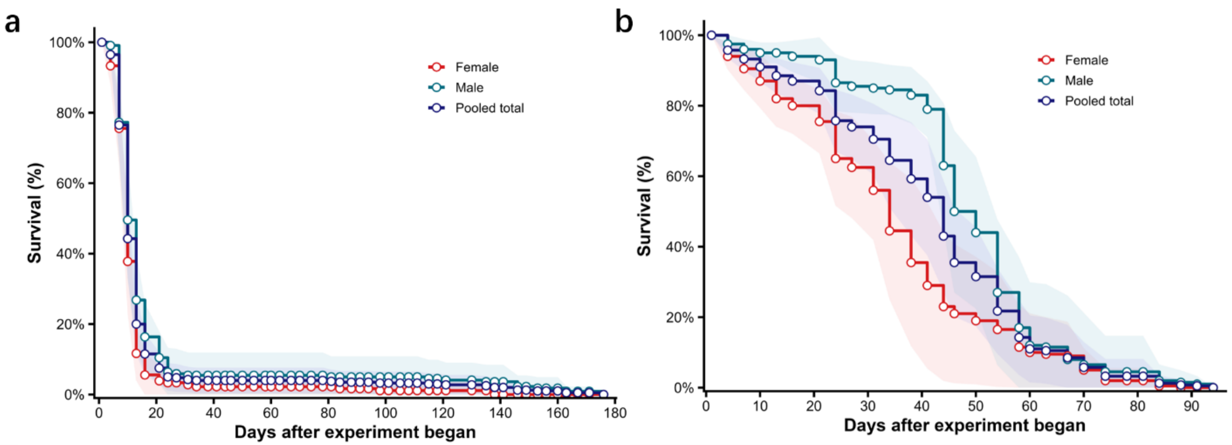

Fig. S3 Survival of male and female *D. immigrans* under two temperature conditions. (a) Survival at 4°C. Lines and open circles show the mean proportion of surviving flies in male (n = 11 vials), female (n = 9 vials), and pooled total (n = 20 vials) groups. (b) Survival at 23°C. Lines and open circles show the mean proportion of surviving flies in male (n = 10 vials), female (n = 10 vials), and pooled total (n = 20 vials) groups. Shaded bands indicate 95% confidence intervals calculated from variation among vials. Each vial initially contained 20 flies, and surviving flies were counted at 3–4-day intervals. Data processing and visualization were performed in R version 4.6.1 using ggplot2 (Wickham 2016; Team 2026).

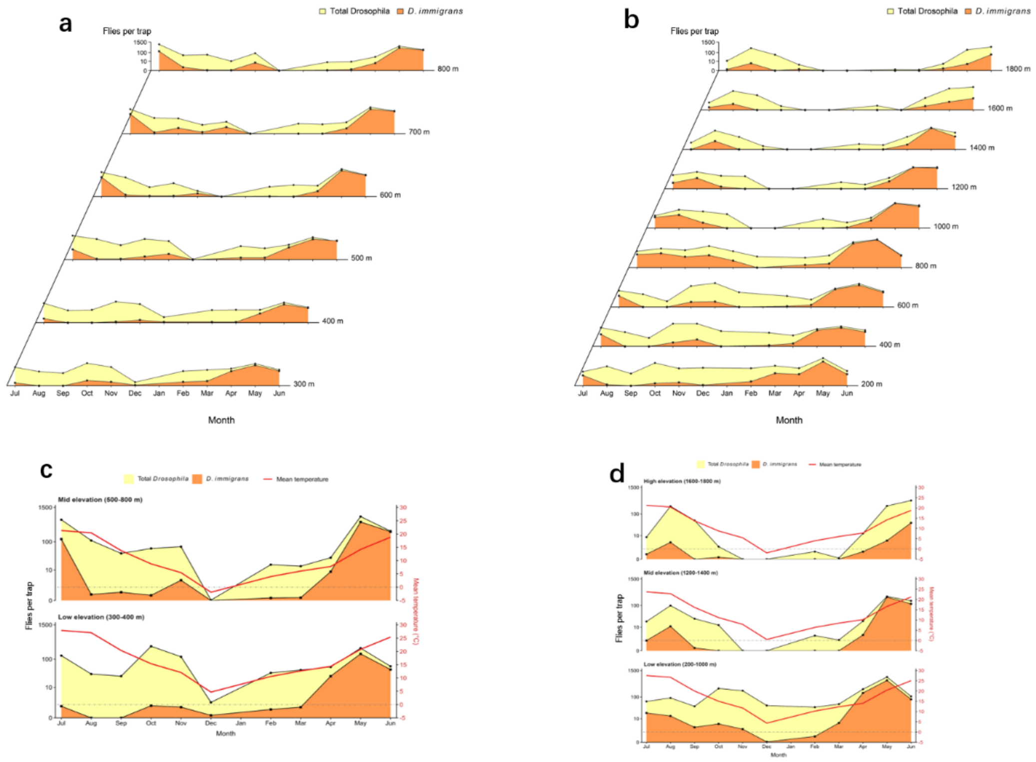

Fig. S4 Seasonal and altitudinal variation in *Drosophila immigrans* abundance at two study sites. (a, b) Monthly mean catches per trap at individual elevations in Langshan (a) and Shunhuangshan (b), Xinning County, Hunan, China. (c, d) Catches pooled within elevation bands at Langshan (300–400 and 500–800 m; c) and Shunhuangshan (200–1000, 1200–1400 and 1600–1800 m; d), with estimated monthly mean temperature. Pale yellow and orange areas represent total drosophilid catches and *D. immigrans*, respectively; *D. immigrans* is included in the total. Catch values are displayed on a log10(n + 1) scale. Flies were collected using fermented banana yeast traps over 48-h intervals; January was not sampled. Lines connect December and February without estimating January catches. Red lines indicate temperature estimated from local meteorological records using a lapse rate of 0.6 °C per 100 m; dash-dotted lines indicate 0 °C. These seasonal shifts in abundance across elevations are consistent with seasonal altitudinal movement of *D. immigrans*. Figures were generated in R (Team 2026), using base graphics and ggplot (Wickham 2016).

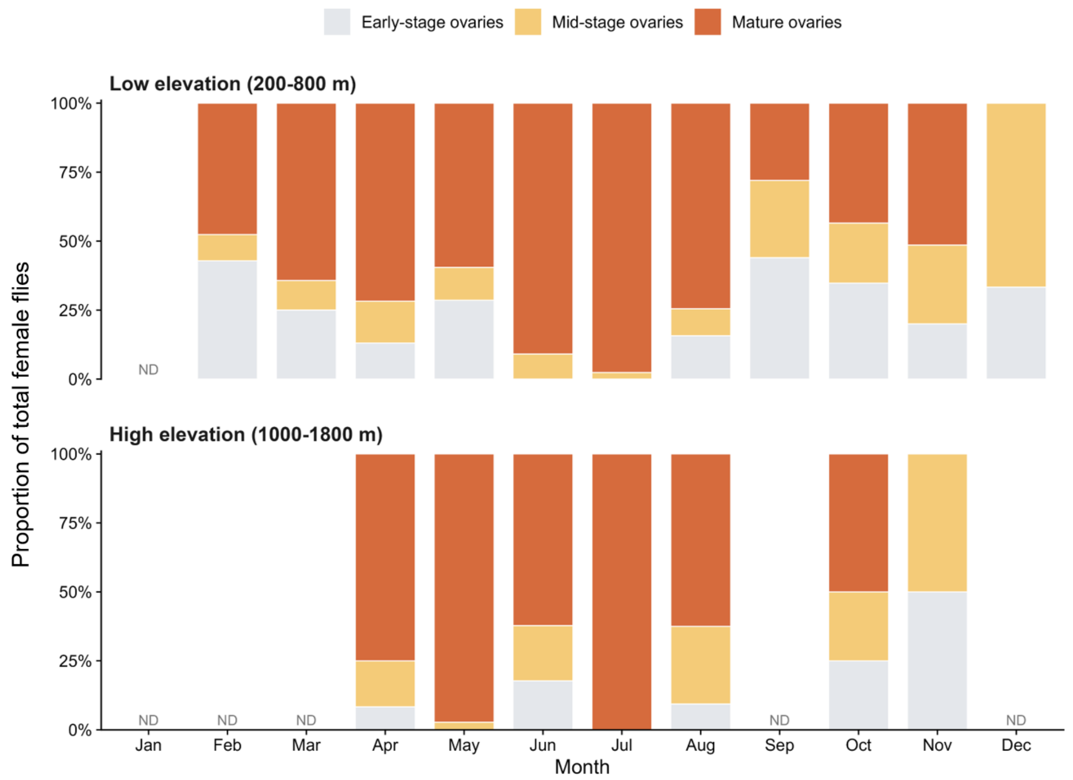

Fig. S5 Seasonal variation in ovarian development of *Drosophila immigrans* at low and high elevations. Monthly proportions of dissected females with early-stage, mid-stage and mature ovaries at low (200–800 m; upper panel) and high (1000–1800 m; lower panel) elevations. Ovarian categories were assigned from egg-chamber morphology and oocyte development, corresponding to stages 1–6, 7–10 and 11–14, respectively, using the staging framework described by Spracklen (Spracklen and Tootle 2013). Grey, yellow and orange indicate the three categories, respectively. Proportions sum to 100% within each sampled elevation–month group. ND, no data available. Figures were generated in R (Team 2026), using base graphics and ggplot (Wickham 2016).

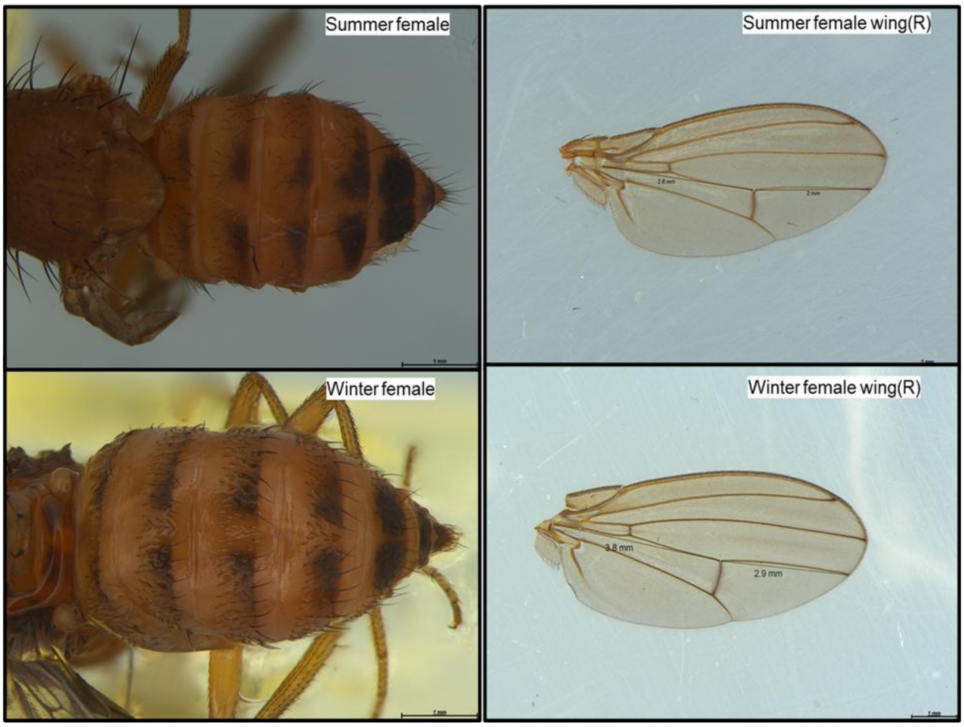

Fig. S6 Representative morphology of summer- and winter-morph female *Drosophila immigrans*. Dorsal abdominal views (left) and dissected right wings (right) of representative summer-morph (upper row) and winter-morph (lower row) females. Specimens were collected at 800 m in Shunhuangshan, with summer samples collected in July and winter samples in November, December and February. Wing length was measured as the summed lengths of two segments along the fourth longitudinal vein, following the measurement approach of Shearer et al. (Shearer et al. 2016). Scale bars, 1 mm. The illustrated winter-morph female has a larger wing than the summer-morph female.

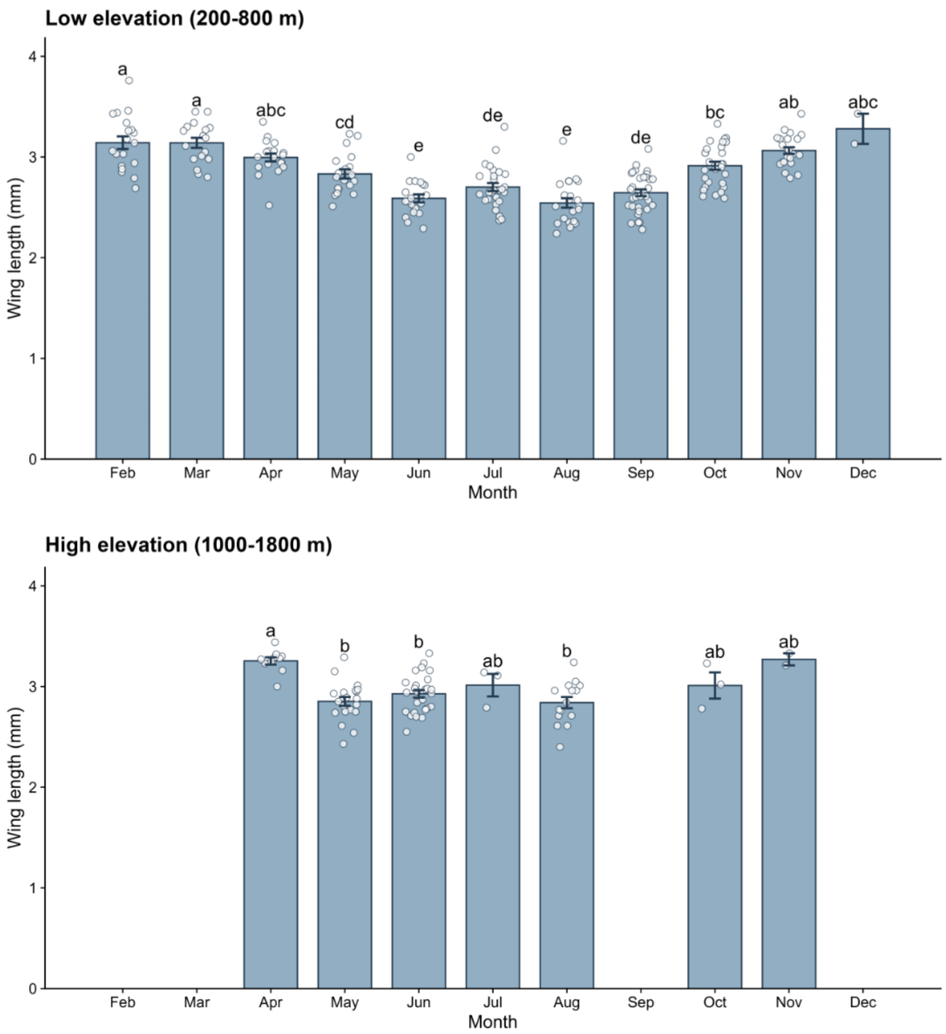

Fig. S7 Seasonal variation in wing length of *Drosophila immigrans* at low and high elevations. Monthly wing lengths at low (200–800 m; upper panel) and high (1000–1800 m; lower panel) elevations, with females and males pooled. Wing length was used as a proxy for body size (Shearer et al. 2016). Bars show means, open circles represent individual flies, and error bars indicate SE. Monthly differences were tested separately within each elevation band using one-way ANOVA followed by Tukey's multiple comparisons. Months without a shared lowercase letter differ significantly (adjusted $P < 0.05$). Blank months indicate no captures; January is omitted. Wing length generally increased during cooler months and decreased during summer, indicating seasonal variation in the body size of captured flies. Monthly differences were analysed using one-way ANOVA followed by Tukey's multiple comparisons in R (Team 2026). Figures were generated using ggplot2 (Wickham 2016), and significance letters were assigned using multcompView (Fox and Weisberg 2019; Graves et al. 2026).

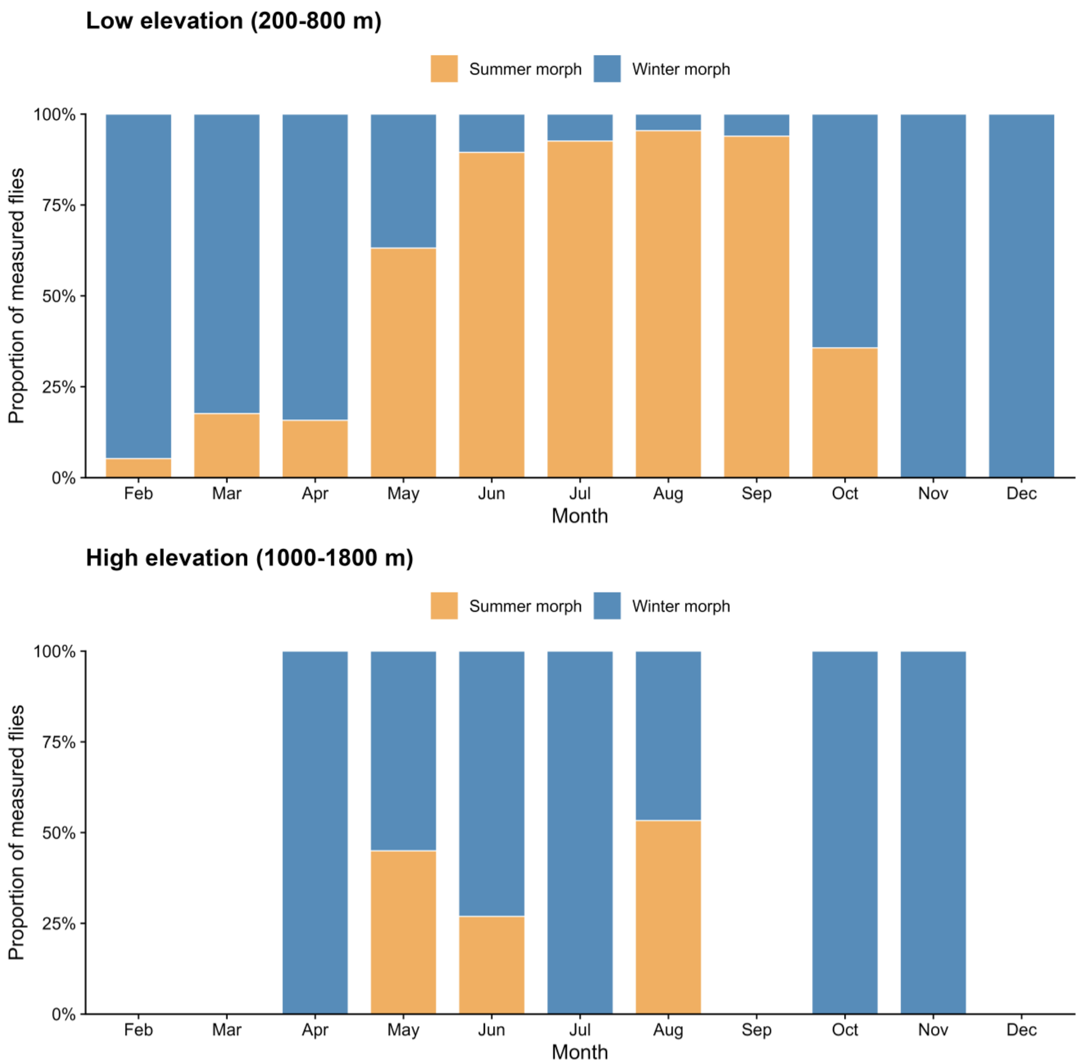

Fig. S8 Seasonal proportions of summer and winter morphs of *Drosophila immigrans* at low and high elevations. Monthly morph composition at low (200–800 m; upper panel) and high (1000–1800 m; lower panel) elevations. Individuals were classified using fixed, sex-specific wing-length thresholds: males <2.74 mm and females <2.94 mm were assigned to the summer morph; individuals at or above these thresholds were assigned to the winter morph. Female and male counts were then pooled to calculate monthly proportions. Orange and blue represent summer and winter morphs, respectively. Blank months indicate no captures; January is omitted. These thresholds define the operational size classes used in this study. Winter morphs predominated during cooler months, whereas summer morphs were more prevalent during summer, particularly at low elevations. Figures were generated in R (Team 2026), using base graphics and ggplot (Wickham 2016).

Fox J and Weisberg S. 2019. An R Companion to Applied Regression, https://socialsciences.mcmaster.ca/jfox/Books/Companion/, 3rd edn. SAGE Publications, Inc., Thousand Oaks, CA

Graves S, Piepho H-P, Selzer L. 2026. multcompView: Visualizations of Paired Comparisons. In, 0.1-11 edn, https://CRAN.R-project.org/package=multcompView

Shearer PW, West JD, Walton VM, et al. 2016. Seasonal cues induce phenotypic plasticity of Drosophila suzukii to enhance winter survival. BMC Ecology 16 (1). 10.1186/s12898-016-0070-3

Spracklen AJ and Tootle TL. 2013. The utility of stage-specific mid-to-late Drosophila follicle isolation. JoVE (Journal of Visualized Experiments), (82):e50493

Team RC. 2026. R: A Language and Environment for Statistical Computing. In. R Foundation for Statistical Computing, Vienna, Austria, https://www.R-project.org/

Wickham H. 2016. ggplot2: Elegant Graphics for Data Analysis10.1007/978-3-319-24277-4. Springer-Verlag, New York, NY